Decay of bound states in oscillating potential wells

Steffen Weimann,[1] Toni Eichelkraut,[2] and Alexander Szameit[1]
[1]*Institut für Physik, Universität Rostock, 18059 Rostock, Germany*
[2]*Carl Zeiss Microscopy GmbH, 07745 Jena, Germany*

(Received 26 February 2018; published 29 May 2018)

In this paper, we report the analytic solution of the oscillating box potential. We investigate the temporal dependence of the amplitude of the ground state as a function of the system parameters. Our analysis reveals the counterintuitive behavior that the loss of the ground state is a nonmonotonic function of the oscillation frequency. On the basis of optical waveguides, we provide an experimental verification of our theoretical findings.

DOI: 10.1103/PhysRevA.97.053844

I. INTRODUCTION

$\mathcal{PT}$ symmetry, as a peculiar extension of conventional quantum mechanics [1], entered optics a few years ago [2,3]. Although originally based on a sensitive interplay of gain and loss [4–6], it turned out that also systems without gain exhibit features that can be associated with $\mathcal{PT}$ symmetry [7–11]. A particular approach to realize appropriate losses in arrays of evanescently coupled femtosecond-laser written waveguides is to undulate the waveguides, in order to generate radiation losses [12].

Due to the well-known quantum-optical analogy [13], an undulated waveguide corresponds to a box potential that is oscillating in time. Although very simple in nature, surprisingly there exists no full analytic solution to this problem. This is somewhat cumbersome, as oscillating box potentials are ubiquitous to many fields in physics, including light-matter interactions [14,15] and waveguide optics [12]. In our work, we tackle this issue and provide an analytic solution of the bound electric field in an oscillating box potential possessing one bound mode only. We note that assuming only one bound mode is not an approximation but rather exactly the situation one finds in single-mode sinusoidal waveguides. The presence of many bound modes might lead to interesting resonances [15]; however, such a treatment goes beyond the scope our current work.

From an analytical point of view, one wants to derive a solution for the temporal evolution of the wave function that acts as the instantaneous ground state of an oscillating potential (illustrated in Fig. 1). At first glance, one might wish to apply Fermi's golden rule [16,17] in order to retrieve the exponential decay rate. However, there are several inadequacies that lie therein. By just applying Fermi's rule, one would simply postulate an exponential decay of the ground-state population. This procedure could neither serve as a rigorous proof of the average exponential decay nor provide the corrections to this average behavior. As a matter of fact, throughout the literature, a number of authors [18–24] have criticized the mathematical grounds of Fermi's derivation, presented generalizations, and even showed the invalidity in certain scenarios. Hence we cautiously avoid Fermi's golden rule and present a careful derivation based on first principles. The following considerations shall concern potential oscillations of the form

$$x_0(z) = d[1 - \cos(\omega z)],$$

where d and ω are the amplitude and frequency of the oscillation, respectively. Although we will treat the exemplary box potential, the findings can be generalized, in principal, to an arbitrary potential. We consider a moving frame of reference in which the potential is stationary again. The one-dimensional (1D) Schrödinger equation for the field $\Psi(x,z)$ is transformed according to

$$\xi = x - x_0(z), \quad \zeta = z,$$

and in the new frame of reference the Schrödinger equation becomes

$$i\partial_\zeta \Psi = -\partial_\xi^2 \Psi + V(\xi)\Psi - i\omega d \sin(\omega\zeta)\partial_\xi \Psi. \qquad (1)$$

All further calculations will be carried out in this frame of reference. Equation (1) represents a 1D Schrödinger equation equipped with a static potential V and an additional oscillating term. It is interesting to note that Eq. (1) can equivalently be transformed to a similar form where the term $i\omega d \sin(\omega\zeta)\partial_\xi$ is replaced by $\omega^2 d \cos(\omega\zeta)\xi$. Applying this so-called Kramers-Henneberger transformation, the equation is well known in many fields of physics, as it represents the dynamics of an electronic wave function under the influence of an external electric field. In a recent publication [12], Eq. (1) was studied numerically in the context of optical waveguides. It was found that when $\Phi_b(x)$ corresponds to the instantaneous ground state of the oscillating potential, then the overall decay of the population of $\Phi_b(x)$ can well be approximated as being exponential. Moreover, the simulations verified the intuition that the decay rate vanishes for very small as well as for high oscillation periods p. For moderate oscillation frequencies, however, the decay rate shows a distinct maximum. An important qualitative finding is that the decay is negligibly small as long as the oscillation period of the potential is smaller than the phase oscillation period of the state $\Phi_b(x)$ of the constant box potential. At this specific frequency the exponential decay suddenly starts to increase. Our analytical solution provides deeper insight into the dependence of the evolution dynamics on the system's parameters and reveals a variety of surprising

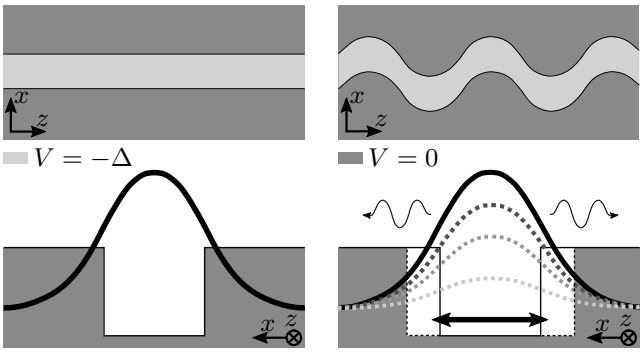

FIG. 1. Sketch of an oscillating box potential with the evolution of the instantaneous fundamental mode of the potential.

properties. In a simple optical experiment we are able to demonstrate the main features of our analysis.

II. THEORETICAL SECTION

In this paper, Eq. (1) is solved analytically using perturbation theory. Assuming ωd to be small, the perturbation term is readily linear in this parameter. In this sense, the general solution strategy is to expand the field Ψ in terms of the modes of the static potential and to perform a first-order perturbation approximation afterwards. In Appendix A we have exhaustively revisited the properties of the modes of the static box potential

$$V = \begin{cases} -\Delta, & |\xi| < a, \\ 0, & \text{else.} \end{cases}$$

Throughout our analysis, we will assume that the potential exhibits only one bound state with transverse mode profile $\Phi_b(x)$ and an eigenvalue ω_b. Having this in mind, the field can be written as

$$\Psi(\xi,\zeta) = c_b(\zeta)\Phi_b(\xi)\, e^{i\omega_b\zeta} + \int_0^\infty [c_s(\zeta,\nu)\Phi_s(\xi) + c_a(\zeta,\nu)\Phi_a(\xi)]e^{i\nu\zeta}d\nu,$$

where for each frequency $\nu > 0$ there is one symmetric mode, $\Phi_s(\xi)$, and one antisymmetric mode, $\Phi_a(\xi)$, in the continuous spectrum. The coefficients c represent yet unknown coefficients which vary with propagation distance ζ. At this point the goal of the analysis is to find the ζ dependence of the coefficient c_b, which represents the amplitude of the bound mode. We want to show that, to first order, c_b is given by an exponential decay, i.e., $c_b \sim e^{-\Gamma\zeta}$. Inserting $\Psi(\xi,\zeta)$ into Eq. (1) and projecting it onto each of the eigenmodes of the straight waveguide one obtains the system of coupled equations

$$\begin{aligned} \partial_\zeta c_b &= \omega d\, \sin(\omega\zeta) \int_0^\infty c_a I_{ba} e^{i\omega_{ab}\zeta} d\omega_a, \\ \partial_\zeta c_s &= \omega d\, \sin(\omega\zeta) \int_0^\infty c_a I_{sa} e^{i\omega_{as}\zeta} d\omega_a, \\ \partial_\zeta c_a &= \omega d\, \sin(\omega\zeta) \left\{ c_b I_{ab} e^{i\omega_{ba}\zeta} + \int_0^\infty c_s I_{as} e^{i\omega_{sa}\zeta} d\omega_s \right\}, \end{aligned} \tag{2}$$

which links the ζ-dependent coefficients c_i. In this system of equations the dependence on the transverse coordinate is eliminated and implicitly expressed in the overlap integrals $I_{ij} = \frac{\langle\Phi_i|\partial_\xi|\Phi_j\rangle}{\|\Phi_i\|^2}$; we also abbreviate $\omega_{ij} = \omega_i - \omega_j$, where $i,j \in \{a,b,s\}$.

At this point, it is necessary to fix the set of initial conditions. Here, we treat the case of $c_a(\zeta = 0) = c_s(\zeta = 0) = 0$ and $c_b(\zeta = 0) = 1$, which represents the fact that initially all light is confined in the bound mode. Despite the change of coordinates, for $d = 0$ we always find $c_b = 1$. The equations for c_a and c_s can now be formally integrated. From this, one gets c_a and c_s, which can be iteratively inserted into the first equation of the system Eq. (2). Following this strategy one obtains an integro-differential equation for the coefficient c_b. In the spirit of first-order perturbation theory subsequently all terms with $(\omega d)^4$ or higher powers of the perturbation parameter will be neglected. This poses a joined condition on the oscillation frequency and amplitude, namely $\omega d \ll 1$. With this the equation for c_b reduces to

$$\begin{aligned} \partial_\zeta c_b &= \omega^2 d^2 \sin(\omega\zeta) \int_0^\infty g(\omega_a) d\omega_a, \\ g(\omega_a) &:= \int_0^\zeta \sin(\omega\tau) c_b(\tau) I_{ab} I_{ba} e^{i\omega_{ba}\tau} e^{i\omega_{ab}\zeta} d\tau. \end{aligned} \tag{3}$$

Up to this point, considering Eq. (3), neither the explicit shape of the modes nor the structure of the perturbation operator have been used. Hence Eq. (3) can be considered as a general expression for any sinusoidally oscillating potential. In order to further simplify and even solve Eq. (3) the kernel of the integral needs to be evaluated:

$$\begin{aligned} I_{ab} I_{ba} &= -\frac{|\langle\Phi_b|\partial_\xi|\Phi_a\rangle|^2}{\|\Phi_b\|^2\|\Phi_a\|^2} = -\alpha S(\omega_a), \\ \alpha &:= \frac{2\Delta^2(\omega_b+\Delta)\kappa_2\cos^2(\kappa_1 a)}{\pi[\Delta\cos^2(\kappa_1 a) + (\omega_b+\Delta)\kappa_2 a]}, \\ S(\omega_a) &:= \frac{k_2 \sin^2(k_1 a)}{\omega_a + \Delta\cos^2(k_1 a)} \frac{1}{(\omega_a - \omega_b)^2}, \end{aligned} \tag{4}$$

where $\kappa_1 = \sqrt{\omega_b + \Delta}$, $\kappa_2 = \sqrt{-\omega_b}$, $k_1 = \sqrt{\omega_b + \omega_a + \Delta}$, and $k_2 = \sqrt{\omega_b + \omega_a}$. Note that α is a constant factor with respect to the integration in Eq. (3) as it only depends on parameters of the static potential. Furthermore, it is assumed that in Eq. (4) one has $k_{1/2} = k_{1/2}(\omega_a)$. Continuing the analysis of Eq. (3) it is advantageous to reverse the order of integration and rewrite it as

$$\begin{aligned} \partial_\zeta c_b &= -\alpha\omega^2 d^2 \sin(\omega\zeta) h(\zeta), \\ h(\zeta) &:= \int_0^\zeta \sin(\omega(\zeta-\tau)) c_b(\zeta-\tau) \int_0^\infty S(\omega_a) e^{i\omega_{ab}\tau} d\omega_a d\tau, \end{aligned} \tag{5}$$

where Eq. (4) as well as the substitution $\tau = \zeta - \tau$ was used. Investigating the temporal behavior of the kernel $\int_0^\infty S(\omega_a) e^{i\omega_a\tau} d\omega_a$ numerically, one finds that it differs only significantly from zero in a very small interval $\tau < \tau_c$. Moreover, in this interval, c_b is only slowly varying and, hence, can

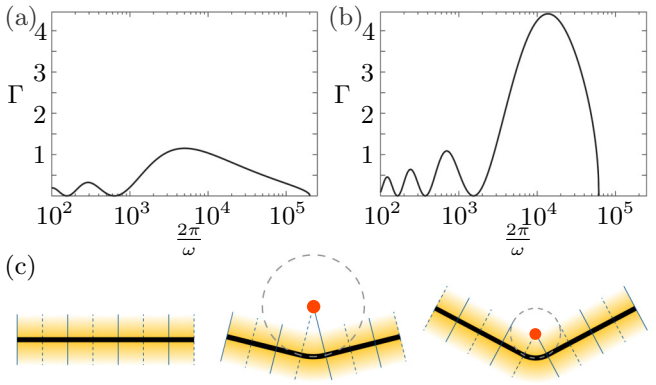

FIG. 2. Exponential decay rate as a function of the potentials oscillation period: (a) analytical solution for $a = 31.271$, $\Delta = 2.0 \times 10^{-4}$, $d = 24.51 \times 10^4$; (b) analytical solution for $a = 48.175$, $\Delta = 2.82 \times 10^{-4}$, $d = 24.51 \times 10^4$. (c) Sketch of how a phase singularity is created by a curved waveguide.

be regarded as constant around $\tau \approx 0$, i.e.,

$$c_b(\zeta - \tau) \approx c_b(\zeta).$$

With the same argument, the upper limit of the temporal integration in Eq. (5) can be extended to infinity. Under this approximation, the differential Eq. (5) can be solved to find the exponential decay of c_b (see Appendix B for a detailed explanation):

$$c_b \sim \exp\left\{-\frac{\pi\alpha\omega^2 d^2}{4}\tilde{S}(\omega_b+\omega)\zeta\right\},$$
$$\tilde{S}(\omega_b+\omega) := \begin{cases} S(\omega_b+\omega), & \omega \geqslant |\omega_b|, \\ 0, & \omega < |\omega_b|. \end{cases} \tag{6}$$

Inserting the argument $\omega_b + \omega$ into the definition of S in Eq. (4) one finds that the exponential decay rate can be written as

$$\Gamma = \begin{cases} \frac{\pi\alpha d^2}{4}\frac{k_2 \sin^2(k_1 a)}{\omega_b+\omega+\Delta\cos^2(k_1 a)}, & \omega \geqslant |\omega_b|, \\ 0, & \omega < |\omega_b|, \end{cases} \tag{7}$$

where, as before, $k_1 = \sqrt{\omega_b+\omega+\Delta}$, $k_2 = \sqrt{\omega_b+\omega}$, and $c_b \sim e^{-\Gamma\zeta}$.

Figures 2(a) and 2(b) display the exponential decay rate as a function of the oscillation period $2\pi/\omega$. The most prominent feature is the vanishing decay for oscillation periods larger than the $2\pi/\omega_b$. In this regime no loss occurs, i.e., the bound state can follow the oscillating potential in an adiabatic manner. The sharp transition between the lossless and the lossy regime can be attributed to the physical fact that light is scattered into only one radiation mode. As a second prominent feature, several nodes appear towards smaller oscillation periods. A very intuitive explanation is based on Fig. 2(c) which illustrates the creation of a phase singularity being associated with every curved region of the waveguide. A curvature strong enough to bring the singularity inside the evanescent field of the guided mode causes a strong perturbation and hence scattering of the guided field into the bulk. In a sinusoidal waveguide, light is radiated away from each bent. Hence, in Fig. 2(a), each minimum corresponds to a situation in which light, that is emitted from successive bends, interferes destructively.

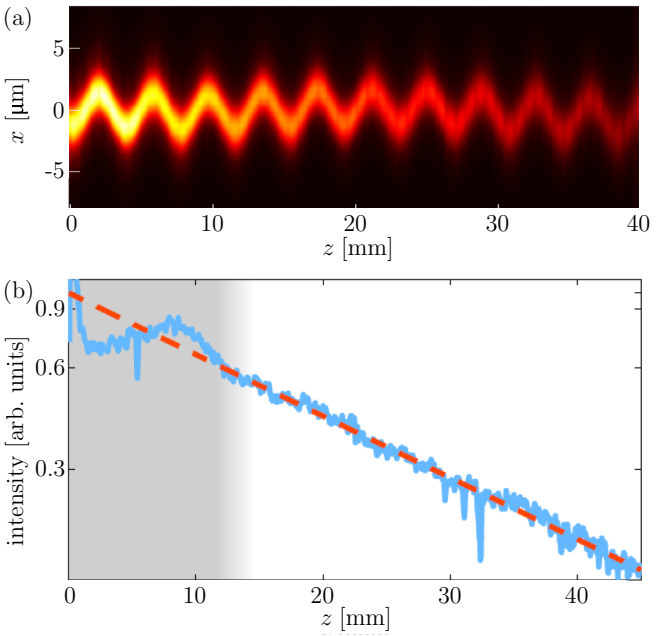

FIG. 3. (a) Fluorescence image of a sinusoidally bent waveguide with an oscillation period of 3.9 mm. (b) Light intensity extracted from the sinusoidally bent waveguide with a period of 3.9 mm (blue line). The red line indicates the extracted decay rate and serves as a guide for the eye.

Intuitively, this behavior can be compared to light scattering at a diffraction grating. Intuitively, this behavior relates to the scattered light leaving the waveguide in a tagential direction. On top of the appearance of extrema, Figs. 2(a) and 2(b) show a transition to a lossless scenario at very short periods. In this limit, the bound mode cannot follow the oscillation, meaning that the fast oscillating potential constitutes an effective z-independent potential. In this regime the loss has to be zero although the eigenvalue of the bound mode is not ω_b anymore. Appendix C provides a mathematical treatment of this regime.

III. EXPERIMENT IN LASER-WRITTEN GLASS WAVEGUIDES

Our experimental results described in the following will demonstrate the main features of our analytical solution, that is, a cutoff frequency, zero loss for at least one frequency higher than the cut-off frequency, as well as the existence of a maximum loss. As we choose a sinusoidally bent waveguide as the oscillating potential, the decay predicted above is manifested as loss of the guided light in the waveguide. In this optical system, the eigenvalues of the modes are represented by propagation constants, whereas the potential is given by the refractive index landscape. The evolution coordinate, ζ, is in the paraxial approximation simply equal to the propagation distance of the light in the waveguide multiplied by $k_0 = 2\pi/\lambda$, where λ is the light wavelength in vacuum [25]. Note that the real transverse coordinate is $\xi/(k_0\sqrt{2n_s})$, the real oscillation frequency is ωk_0, and the real oscillation amplitude is $d/(k_0\sqrt{2n_s})$. In Fig. 3(a) an exemplary evolution of the light intensity at a wavelength of $\lambda = 633$ nm inside an oscillating waveguide is shown, obtained using a fluorescence microscopy

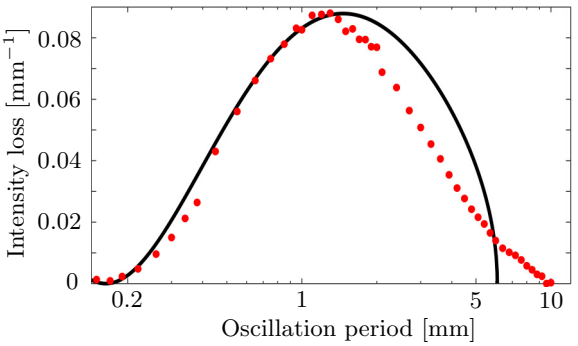

FIG. 4. Experimentally measured intensity decay rate (red dots) and decay rate Γ (black line) plotted for a step index waveguide with index step $\Delta = 2.80 \times 10^{-4}$, full waveguide width $2a/(k_0\sqrt{2n_s}) = 5.84\ \mu$m, and a real oscillation amplitude of $d/(k_0\sqrt{2n_s}) = 1.45\ \mu$m. The substrate refractive index of our samples is 1.45.

technique [26]. We fabricated several samples with period lengths ranging from 200 μm to 50 mm using the fs-laser writing technology [27]. All samples share a common length of 50 mm as well as a sine amplitude of $d = 1.45\ \mu$m. For the measurements, from which the light amplitude is extracted, the waveguide oscillates orthogonal with respect to the focal plane of the imaging objective [in contrast to Fig. 3(a) that was taken only for illustration purposes]. In Fig. 3(b), we plot an exemplary intensity decay in an oscillating waveguide (blue line), extracted from a fluorescence image, for a waveguide modulation period of 3.9 mm. After a propagation distance of 12 mm the graph clearly shows a linear slope due to the logarithmic scaling of the axis of ordinates (red dotted line), indicating the exponential decay of the light intensity. Notably, for propagation distances smaller than 12 mm, the measured intensity deviates from the exponential behavior obtained for larger propagation distances due to imperfect mode overlap between the guided mode and the incoupling objective. Consequently, in all samples this region was not taken into account when evaluating the decay rate. In the particular example shown in Fig. 3(b) the slope is -0.42 cm^{-1}. In Fig. 4 we plot the intensity decay rates as a function of the oscillation period extracted from experimental data (red dots) and compare them to our analytic 1D theory (black line). For large period lengths >10 mm the extracted decay rate of 0.011 mm^{-1} does not differ significantly from the intrinsic decay of the straight waveguides, which originates from the fabrication process. Additionally, for very short periods $\approx$ 200 μm, the extracted decay rate is also essentially equivalent to the intrinsic decay in a straight waveguide. For intermediate oscillation periods between 200 μm and 6 mm, the measured data shows the predicted behavior. There indeed exists a single maximum loss of 1.0 cm^{-1}, at a period length of 1.2 mm, exceeding the intrinsic waveguide loss for more than one order of magnitude.

Importantly, we would like to point out that the experimental results differ slightly from the analytic solution, presented in Fig. 2: the theoretically predicted sudden drop in the decay rates for increasing oscillation periods is slightly smoother in the experiment. This deviation between theory and experiment can be attributed to the underlying dimensionality. While the experimental waveguides exhibit a 2D cross section, the analytical model describes only one transverse dimension. In contrast to the 1D model, a continuum of radiation modes is excited at each bent and the sharp transition between the lossless and the lossy region is smeared out.

In conclusion, we presented an analytic theory of an oscillating potential and use our results to predict and explain the loss behavior in modulated waveguides. We find that there is virtually no additional loss in the waveguides for small and high modulation frequencies, respectively, beyond their intrinsic loss. For intermediate modulation frequencies, however, the decay rate increases and a single pronounced maximum can be observed. The results presented in this paper form the basis of subsequent investigations, since they prove that sinusoidally bent waveguides can be experimentally applied to mimic lossy media. With this, it enables the implementation and study of $\mathcal{PT}$-symmetric and other dissipative structures. Certainly, the investigation of oscillating potential wells with several bound modes is also interesting, as these states might cause complex resonances. This problem will be treated in future work.

ACKNOWLEDGMENTS

This research was supported by the Deutsche Forschungsgemeinschaft (Grants No. SZ 276/9-1 and No. SZ 276/15-1).

S.W. and T.E. contributed equally to this work.

APPENDIX A: STRAIGHT WAVEGUIDE REVISITED

This first section revisits the well-known case of a 1D Schrödinger equation,

$$i\,\partial_t \Psi(x,t) = -\partial_x^2 \Psi(x,t) + V(x)\Psi(x,t),$$

with the time-independent box potential

$$V(x) = \begin{cases} -\Delta, & |x| \leqslant a, \\ 0, & |x| > a, \end{cases}$$

where Δ and a are positive real constants representing the potential's depth and width, respectively. The fundamental mode is given by

$$\Phi_b = \begin{cases} \cos(k_1 a) e^{\sqrt{-\omega_b}(\xi+a)}, & \xi < -a, \\ \cos\left(\sqrt{V_0+\omega_b}\xi\right), & |\xi| < a, \\ \cos(k_1 a) e^{-\sqrt{-\omega_b}(\xi-a)}, & \xi > a. \end{cases}$$

For the unbound symmetric modes one finds

$$\Phi_s(\xi,\beta) = \begin{cases} \mathrm{Re}\left\{A_s e^{-ik_2(\xi+a)}\right\}, & \xi < -a, \\ \cos(k_1\xi), & |\xi| < a, \\ \mathrm{Re}\left\{A_s e^{ik_2(\xi-a)}\right\}, & \xi > a, \end{cases}$$

and the unbound, antisymmetric modes are

$$\Phi_a(\xi,\beta) = \begin{cases} -\mathrm{Re}\left\{A_a e^{-ik_2(\xi+a)}\right\}, & \xi < -a, \\ \sin(k_1\xi), & |\xi| < a, \\ \mathrm{Re}\left\{A_a e^{ik_2(\xi-a)}\right\}, & \xi > a. \end{cases}$$

In these formulas we have used

$$A_s := \cos(k_1 a) + i\frac{k_1}{k_2}\sin(k_1 a),$$

$$A_a := \sin(k_1 a) - i\frac{k_1}{k_2}\cos(k_1 a),$$

$$k_1 := \sqrt{\Delta + \omega},$$

$$k_2 := \sqrt{\omega},$$

where $\omega \geqslant 0$. The normalization of the modes is given by

$$\langle \Phi_{a/s}(\nu)|\Phi_{a/s}(\nu')\rangle = 2\pi k_2 |A_{a/s}|^2 \delta(\nu - \nu')$$

for the radiation modes and

$$\langle \Phi_b|\Phi_b\rangle = \frac{\cos(\kappa_1 a)}{\kappa_1\kappa_2}[\kappa_1\cos(\kappa_1 a) + \kappa_2\sin(k_1 a)] + a$$

for the bound mode.

APPENDIX B: AUXILIARY STEPS IN THE CALCULATION OF THE DECAY RATE Γ

The term $\sin(\omega(\zeta - \tau))$ in Eq. (5) of the main text is not slowly varying within the interval $0 < \tau < \tau_c$ and has to be fully considered. Integration of Eq. (5) with respect to τ and finally ω_a yields

$$\partial_\zeta c_b = \alpha\omega^2 d^2 c_b(\zeta)\Big[\sin(\omega\zeta)T(\omega_b,\omega) + \frac{\sin(2\omega\zeta)}{2}U(\omega_b,\omega)\Big],$$

$$T(\omega_b,\omega) := \frac{\pi\tilde{S}(\omega_b+\omega)}{2} - i\mathcal{P}\int_0^\infty \frac{(\nu-\omega_b)S(\nu)}{(\nu-\omega_b)^2-\omega^2}d\nu,$$

$$U(\omega_b,\omega) := \mathcal{P}\int_0^\infty \frac{\omega S(\nu)}{(\nu-\omega_b)^2-\nu^2}d\nu + i\frac{\pi\tilde{S}(\omega_b+\omega)}{2},$$

$$\tilde{S}(\omega_b+\omega) := \begin{cases} S(\omega_b+\omega), & \omega \geqslant |\omega_b|, \\ 0, & \omega < |\omega_b|. \end{cases} \tag{B1}$$

Note that both $T(\omega_b,\omega)$ and $U(\omega_b,\omega)$ are split into real and imaginary parts which is ensured since both $\tilde{S}$ and the integrals are purely real. One last integration of Eq. (B1) yields the final expression for the amplitude of the bound mode within an oscillating potential; it reads

$$c_b = \exp\left\{\frac{\alpha\omega^2 d^2}{2}T(\zeta - \sin(2\omega\zeta)) + \frac{\alpha\omega d^2}{4}U(1-\cos(2\omega\zeta))\right\}.$$

Analyzing the structure of this result one can identify several terms which are qualitatively different. Starting with the second exponential, one finds that it only contributes to a periodic oscillation, whereas the real part of U is responsible for an amplitude oscillation and its imaginary part is responsible for a corresponding phase oscillation. Also the first exponential term contains an oscillating part and equal to the second exponential it consists of both a phase and amplitude oscillation. All oscillating terms in c_b have the same frequency, which corresponds to twice the oscillation frequency of the waveguide. This observation was already made in connection with the simulations in Fig. 3(b) of [12] and hence is in perfect agreement. It is illustrated that the amplitude as well as phase oscillations are only small and can be neglected for long-term evolution. The only term in c_b which contributes to a long-term modulation is $c_b \sim \exp\{\frac{\alpha\omega^2 d^2}{2}T(\omega_b,\omega)\zeta\}$. Since T consists of both a real and an imaginary part, it follows that only one term remains:

$$c_b \sim \exp\left\{\frac{\pi\alpha\omega^2 d^2}{4}\tilde{S}(\omega_b+\omega)\zeta\right\}.$$

APPENDIX C: HIGH-FREQUENCY REGIME

The previous findings, i.e., their validity, are limited to small frequencies, as stated in the main text. It was found before [12] that the loss of a sinusoidally modulated waveguide vanishes for very high frequencies. This section serves as a rigorous proof of the numerical findings in [12], which we call here the high-frequency limit. The starting point of the subsequent analysis shall be the 1D Schrödinger equation with the sinusoidally oscillating potential. In general, the field can be decomposed into its Fourier components as

$$\Psi(x,z) = \int_{-\infty}^{\infty}\tilde{\Psi}(x,\beta)e^{i\beta z}d\beta.$$

If it can be assumed that the spectral width of $\Psi(x,z)$ is limited and there exists a frequency $\beta_{\max}$ for which holds that if $|\beta| > |\beta_{\max}|$ then $\tilde{\Psi}(x,\beta) \approx 0$, then one can find a small longitudinal interval Z with $Z \ll 2/\beta_{\max}$ so that

$$\langle\Psi(x,z)\rangle_z = \frac{1}{Z}\int_{z-\frac{Z}{2}}^{z+\frac{Z}{2}}\Psi(x,z')dz' = \Psi(x,z).$$

This is true, because one can exchange the Fourier integral and the z averaging and then for each Fourier component

$$\frac{1}{Z}\int_{z-\frac{Z}{2}}^{z+\frac{Z}{2}}\tilde{\Psi}(x,\beta)e^{i\beta z'}dz' = \begin{cases}\tilde{\Psi}(x,\beta)e^{i\beta z}, & |\beta| \leqslant |\beta_{\max}|, \\ 0, & |\beta| > |\beta_{\max}|.\end{cases}$$

Applying this moving average to the 1D Schrödinger equation one finds

$$i\partial_z\Psi(x,z) = -\partial_x^2\Psi(x,z) + \langle V(x,z)\rangle_z\Psi(x,z),$$

where it was used that $\langle\partial_z\Psi\rangle_z = \partial_z\langle\Psi\rangle_z$ as well as $\langle\Delta\Psi\rangle_z = \langle\Delta\rangle_z\Psi$, employing the same argument as above. If the frequency ω with which the potential V is oscillating is much larger than $2\pi/Z$, then the mean potential $\langle V\rangle_z$ is constant along the z axis. As a consequence, in this high-frequency limit the field amplitude Ψ only feels a constant potential along the z direction. In general, the shape of the potential changes due to the averaging procedure and it should be stated that $\langle V(x-x_0)\rangle \neq V(x-\langle x_0\rangle_z)$. Instead, for a box potential with the specific parameters $d = 1\ \mu$m and $a = 3\ \mu$m the potential is depicted in Fig. 5. In general, due to the average potential being different from the original

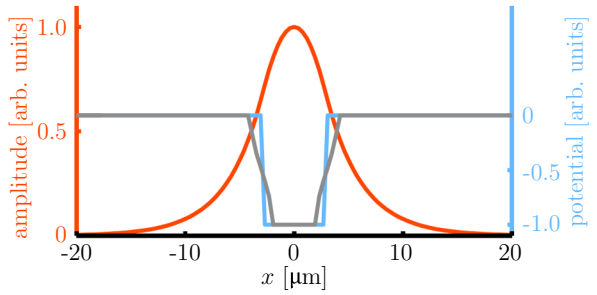

FIG. 5. Comparison between straight waveguide and average potential for high oscillation frequencies with $d = 1\ \mu$m and $a = 3\ \mu$m. The blue line represents the straight box potential, whereas the gray line shows the oscillating average potential. For the parameters under consideration the eigenmode profile of both potentials (red line) is almost identical.

potential also the shape of the bound mode changes. However, for the specific parameters under consideration, both profiles are almost identical. If such an averaged potential is excited with its own bound mode then—in the high-frequency limit—the evolution is stationary and $\Psi(x,z) = \Phi(x)\exp\{i\omega_b z\}$. In this case $\beta_{\max}$ can simply be identified with ω_b and one finds the condition

$$\omega_b \ll \frac{2}{Z} < \frac{2\pi}{Z} \ll \omega,$$

which relates the modulation frequency of the potential with the propagation constant of the bound mode. This condition determines the validity of the high-frequency approximation above, for which the loss of the bound mode is perfectly zero [12].

[1] C. M. Bender and S. Boettcher, Phys. Rev. Lett. **80**, 5243 (1998).
[2] R. El-Ganainy, K. G. Makris, D. N. Christodoulides, and Z. H. Musslimani, Opt. Lett. **32**, 2632 (2007).
[3] K. G. Makris, R. El-Ganainy, D. N. Christodoulides, and Z. H. Musslimani, Phys. Rev. Lett. **100**, 103904 (2008).
[4] C. E. Rüter, K. G. Makris, R. El-Ganainy, D. N. Christodoulides, M. Segev, and D. Kip, Nat. Phys. **6**, 192 (2010).
[5] A. Regensburger, C. Bersch, M.-A. Miri, G. Onishchukov, D. N. Christodoulides, and U. Peschel, Nature **488**, 167 (2012).
[6] M. Wimmer, M.-A. Miri, D. N. Christodoulides, and U. Peschel, Sci. Rep. **5**, 17760 (2015).
[7] M. Ornigotti and A. Szameit, J. Opt. **16**, 065501 (2014).
[8] A. Guo, G. J. Salamo, D. Duchesne, R. Morandotti, M. Volatier-Ravat, V. Aimez, G. A. Siviloglou, and D. N. Christodoulides, Phys. Rev. Lett. **103**, 093902 (2009).
[9] T. Eichelkraut, R. Heilmann, S. Weimann, S. Stuetzer, F. Dreisow, D. N. Christodoulides, S. Nolte, and A. Szameit, Nat. Commun. **4**, 2533 (2013).
[10] M. Golshani, S. Weimann, K. Jafari, M. K. Nezhad, A. Langari, A. R. Bahrampour, T. Eichelkraut, S. M. Mahdavi, and A. Szameit, Phys. Rev. Lett. **113**, 123903 (2014).
[11] S. Weimann, M. Kremer, Y. Plotnik, Y. Lumer, S. Nolte, K. G. Makris, M. Segev, M. C. Rechtsman, and A. Szameit, Nat. Mater. **16**, 433 (2017).
[12] T. Eichelkraut, S. Weimann, S. Stuetzer, S. Nolte, and A. Szameit, Opt. Lett. **39**, 6831 (2014).
[13] S. Longhi, Laser Photon. Rev. **3**, 243 (2008).
[14] Y. B. Zel'dovich, Usp. Fiz. Nauk **110**, 139 (1973).
[15] Z. Chang, *Fundamentals of Attosecond Optics* (CRC Press, Taylor and Francis Group, London, 2011).
[16] E. Fermi, Z. Phys. **88**, 161 (1934).
[17] C. Cohen-Tannoudji, B. Diu, and F. Laloe, *Quantum Mechanics* (Wiley, New York, 1991), Vol. 1.
[18] L. Fonda, G. C. Ghirardi, and A. Rimini, Nuovo Cimento A **25**, 537 (1975).
[19] R. Alicki, Int. J. Theor. Phys. **16**, 351 (1977).
[20] M. Combescot, J. Phys. A **34**, 6087 (2001).
[21] H. M. Pastawski, Physica B (Amsterdam) **398**, 278 (2007).
[22] D. Taj, R. C. Iotti, and F. Rossi, Semicond. Sci. Technol. **24**, 065004 (2009).
[23] J. M. Zhang and Y. Liu, Eur. J. Phys. **37**, 065406 (2016).
[24] D. Dragoman, Phys. Lett. A **274**, 93 (2000).
[25] D. N. Christodoulides and R. I. Joseph, Opt. Lett. **13**, 794 (1988).
[26] A. Szameit, F. Dreisow, H. Hartung, D. Nolte, A. Tünnermann, and F. Lederer, Appl. Phys. Lett. **90**, 241113 (2007).
[27] A. Szameit and S. Nolte, J. Phys. B **43**, 163001 (2010).